American Mineralogist, Volume 76, pages 756–772, 1991

Coronal reaction textures in garnet amphibolites of the Llano Uplift

WILLIAM D. CARLSON, CAMBRIA D. JOHNSON
Department of Geological Sciences, University of Texas at Austin, Austin, Texas 78713, U.S.A.

ABSTRACT

Almandine-rich garnets in mafic amphibolites of the Llano Uplift of central Texas display remarkably well-organized coronal textures with characteristics diagnostic of diffusion-controlled reaction. The garnets have undergone static resorption reactions of three types: (1) reaction with a metamorphic fluid along fractures to produce symmetrical layers of magnetite and symplectitic labradorite + ferroan pargasite; (2) reaction with quartz to produce coronal layers of plagioclase (oligoclase-andesine) + magnetite and orthopyroxene + augite; and (3) reaction with omphacite to produce coronal layers of symplectitic labradorite + ferroan pargasite ± magnetite and magnesio-hornblende + oligoclase ± orthopyroxene. Material-balance calculations assuming volume conservation in an inert-marker reference frame demonstrate that none of these reactions can be considered isochemical. Instead, substantial amounts of Na, Ca, Fe, Mg, Si, and Al must have been transported across the boundaries of the reaction bands.

An open-system diffusion model for the garnet-quartz and garnet-omphacite reaction bands establishes that each of the assemblage zonations observed is stable with respect to diffusion over a substantial range of possible ratios of the phenomenological coefficients for intergranular diffusion. Differences in the relative values for the phenomenological coefficients between the garnet-quartz and garnet-omphacite reaction bands may reflect differences in the chemistry of the intergranular fluid, particularly in the degree of silica saturation. Garnet-omphacite reaction bands exhibit petrographic evidence for the progressive replacement of orthopyroxene by hornblende, indicating that the product assemblage in this reaction band evolved over time. Calculations based on the open-system diffusion model suggest that this temporal evolution results from changes in the amounts of material transported across the boundaries of the reaction band in response to the progress of a reaction (external to the garnet-omphacite corona) in which omphacite breaks down to sodian augite + oligoclase + magnesio-hornblende. To be petrologically valid, models of diffusion-controlled reactions must therefore address rigorously the difficult questions of the degree of chemical exchange of a reaction with its surroundings and the extent to which that exchange may vary as reaction progresses.

INTRODUCTION

The textures of metamorphic rocks reflect in intricate ways the elaborate interplay between the kinetics of intergranular diffusion and the kinetics of other processes essential to recrystallization, such as the rates of breakdown of unstable phases, the rates of nucleation and growth of stable phases, and the rates of change of intensive parameters (cf. Ridley and Thompson, 1986; Carlson, 1989). In some instances, the relative importance of these factors is evident: for example, the kinetic dominance of the diffusion process is expressed with unusual clarity in coronal reaction bands such as those between crystals of olivine and plagioclase in metagabbroic rocks (e.g., Johnson and Carlson, 1990) and in some mineral segregations (e.g., those described by Foster, 1981). Because the kinetics of intergranular diffusion may limit reaction rates even in rocks lacking reaction coronas or mineral segregations (Carlson, 1989), analysis of coronal structures should produce insight into reaction mechanisms that also operate in metamorphic rocks with less exotic textures.

In this work, therefore, we seek a quantitative understanding of the kinetics of intergranular diffusion in coronal reaction bands around garnets in a metagabbro body from the Llano Uplift of central Texas. We use a transport model based in nonequilibrium thermodynamics to analyze the petrographic and compositional features of these coronal textures. In contrast to previous attempts by others to explain analogous textures in terms of steady-state closed-system models, we argue that these textures can be rigorously explained only as the products of diffusion-controlled reactions in an open system in which the local product assemblages may change with time in response to the progress of reactions taking place beyond the confines of any individual coronal reaction band.

0003–004X/91/0506–0756$02.00

Previous work

In this volume honoring J. B. Thompson, Jr., it is fitting to acknowledge that his articulation of the concept of local equilibrium in metasomatic processes, published over 30 years ago (Thompson, 1959), has been the basis for nearly all subsequent attempts to understand diffusion-controlled reaction textures. Thompson's recognition that sufficiently small regions of a rock may approach internal chemical equilibrium, despite the presence of gradients in chemical potential from one such region to another, provides exactly the perspective required to analyze metamorphic reactions for which the kinetics are controlled by rates of diffusion rather than by the rates of dissolution or precipitation at mineral surfaces. This concept of local equilibrium in metasomatic processes makes it possible to link the mineral assemblage and compositions at any point within a reaction band to the chemical potentials at that point, even though the reaction band as a whole is a nonequilibrium system characterized by gradients in the chemical potentials of components in the intergranular medium.

Fisher (1973, 1975, 1977) brought the rigor of nonequilibrium thermodynamics to bear on the quantitative analysis of diffusion-controlled metamorphic processes, and Brady (1977) described important consequences of diffusional processes for metasomatic zones in metamorphic rocks. On this foundation, Joesten (1977) constructed an integrative mathematical formalism for the analysis of the zoning of mineral assemblages during diffusion metasomatism. Joesten's elegant model allows one to evaluate the diffusional stability of a reaction band for any arbitrary set of intergranular diffusion coefficients, knowing only the compositions of the phases involved in the reaction. Features of the reaction band that can be calculated from the model include the relative widths of product layers, their modal proportions, the fluxes of elements across layers in the reaction band, and the stoichiometry of the reactions occurring at each interface between layers in the reaction band. A similar approach, using a somewhat different formalism, has been developed by Foster (1981) and applied to the analysis of mineral segregations in metamorphic rocks (Foster, 1981, 1983, 1986).

Quantitative analysis of diffusion in coronal textures has been restricted so far to the study of reactions between olivine and plagioclase in metagabbroic rocks (Nishiyama, 1983; Joesten, 1986a, 1986b; Grant, 1988; Johnson and Carlson, 1990). The results of these investigations emphasize an important discrepancy: whereas coronal reaction textures observed in rocks commonly exhibit open-system behavior, the diffusion model of Joesten (1977) assumes, for all components with appreciable chemical potential gradients across the reaction band, that no transport of materials beyond the boundaries of the reaction band takes place. Because of this discrepancy, the attempts of Nishiyama (1983) and Grant (1988) to replicate natural olivine-plagioclase reaction textures were not completely successful. Joesten (1986b, p. 479) briefly considered the possibility of open-system behavior by arbitrarily specifying an external flux for a single component in an olivine-plagioclase reaction corona. Johnson and Carlson (1990) extended Joesten's model to fully open systems by specifying, on the basis of material-balance calculations, the magnitudes of all component fluxes beyond the boundaries of reaction bands in olivine-plagioclase coronas in metagabbros of the Adirondack Mountains. With this approach, the two most common types of olivine-plagioclase coronas found in the Adirondacks were modeled successfully, and it was demonstrated that those coronas probably did not originate by a single steady-state diffusion process, but instead evolved with time through one or more transient states.

Although olivine-plagioclase reaction bands are by far the most common and most carefully studied coronal texture, equally well-developed coronas are often found surrounding garnets in mafic amphibolites (e.g., Misch and Onyeagocha, 1976). The coronas around garnet present an intriguing comparison with the olivine-plagioclase coronas insofar as they originate at lower temperatures and pressures, and possibly at higher activities of aqueous fluid; in addition, there is no question of a possible igneous contribution to their origin (cf. Joesten, 1986a). Thus this inquiry into the origin of coronas surrounding garnets in amphibolites of the Llano Uplift allows a test, under different geologic conditions, of the assertion of Johnson and Carlson (1990) that many natural coronal textures can be quantitatively understood only as the consequence of open-system diffusion-controlled reactions.

Occurrence and description of coronal textures

With few exceptions, almandine garnets of the Llano Uplift show textural evidence, compositional evidence, or both, of partial resorption, whether they occur in mafic, pelitic, or semipelitic units. Although almandine garnets in many localities across the uplift are surrounded by roughly concentric zones of plagioclase ± cordierite ± biotite (in pelitic rocks) or plagioclase ± hornblende ± magnetite (in mafic rocks), this article restricts its attention to a single locality, the informally named "Whitt Ranch metagabbro," in which the resorption textures show substantial mineralogic variety and particularly strong spatial organization. The Whitt Ranch metagabbro is considered below in its regional context, and the petrographic and compositional features of the coronal reaction textures found within it are described in detail.

Geologic setting

Regional geology. The Llano Uplift exposes metaigneous and metasedimentary rocks of the Llano Supergroup, for which protolith ages approach 1300 Ma (Walker, 1988). Between ~1167 and ~1080 Ma, the protoliths underwent amphibolite-facies metamorphism at moderate to high pressures (Carlson and Nelis, 1986; Wilkerson

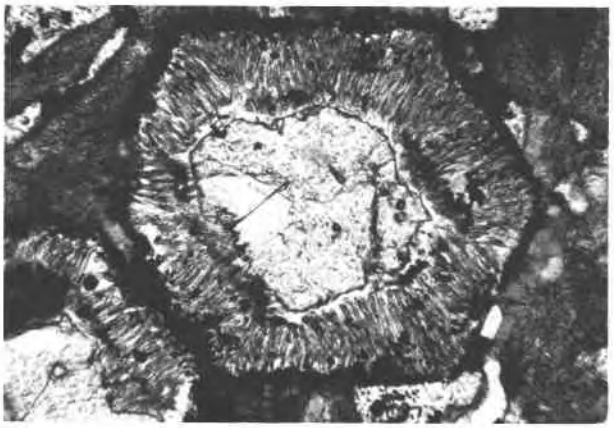

Fig. 1. Photomicrograph of a coronal texture produced by garnet-omphacite reaction. The approximate location of the original surface of a euhedral garnet crystal is now marked by a hexagonal rim of magnetite crystals, separated from central relict garnet by a radial symplectite of amphibole and plagioclase with scattered magnetite crystals. Close to the relict garnet (especially to its right), linear concentrations of magnetite mark the outer boundary of an incomplete concentric secondary corona. Long dimension of image is 1.2 mm.

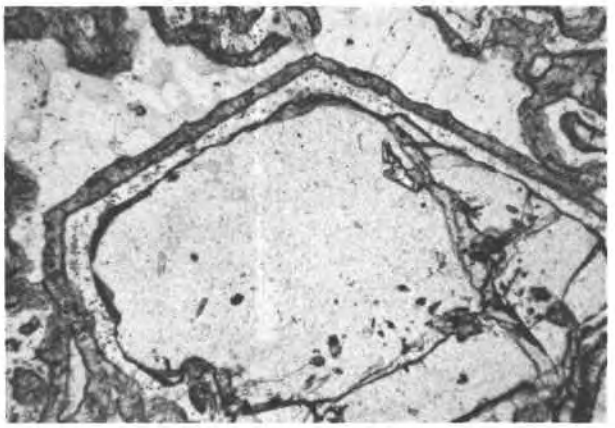

Fig. 2. Photomicrograph of a coronal texture produced by garnet-quartz reaction. Central garnet crystal is separated from polycrystalline quartz by an inner layer of plagioclase speckled by tiny crystals of magnetite and an outer layer of intergrown clinopyroxene and orthopyroxene. Long dimension of image is 4.5 mm.

et al., 1988) accompanied by complex polyphase deformation (Nelis et al., 1989; Carter, 1989). Deformation ceased and the metamorphic rocks rose to shallower levels of the crust before the intrusion of numerous granitic plutons, stocks, and dikes at ~1090–1050 Ma (Zartman, 1964; Garrison et al., 1979). At the time of this intrusive episode, the uplift experienced a regionally extensive reheating and hydration event sufficient to reset K-Ar systems in metamorphic hornblende and biotite (Garrison et al., 1979) and to induce both widespread static recrystallization (Nelis et al., 1989; Carter, 1989) and mineralogic and isotopic reequilibration to fluids genetically linked to the granitic intrusions (Bebout and Carlson, 1986). For a more detailed review of the regional geology of the Llano Uplift and a discussion of related Precambrian rocks in Texas, consult Mosher (in press).

In this regional context, the abundant petrologic evidence for the instability of almandine in the uplift is attributed to a polymetamorphic history in which garnet grew in an early dynamothermal event of moderate to high pressure but was partially resorbed by reaction during a later static metamorphic event at low pressure. Phase equilibria (e.g., Holdaway and Lee, 1977) and field relations elsewhere (e.g., Chesworth, 1972) indicate that garnet-resorption reactions should occur when garnetiferous assemblages in typical pelitic and mafic bulk compositions are reequilibrated at pressures in the range of 2–4 kbar. Such pressures are consistent with barometric estimates for metamorphic assemblages in the uplift whose decussate textures and association with local fluid infiltration clearly indicate growth during the late static metamorphic event (Bebout and Carlson, 1986).

The Whitt Ranch metagabbro. The Whitt Ranch metagabbro body is located approximately 2 km northwest of the community of Baby Head, just northeast of Texas Highway 16, at Universal Transverse Mercator coordinates 14RNK318181. (This locality is entirely on private property. Prior permission must be obtained from the owner before visiting the locality. The senior author will be pleased to provide assistance in contacting the landowner.) Mapping by Jordan (1970) and Moseley (1977) shows the metagabbro body to be an elliptical mass of garnet amphibolite 0.5 by 0.9 km in diameter, completely surrounded by quartzofeldspathic Valley Spring Gneiss. A metasomatic border zone extends inward about 30 m from the contact of the metagabbro with the gneiss; it is characterized by larger grain sizes, by the presence of alkali feldspars, and by the complete replacement of garnet by biotite + plagioclase + amphibole. Alkali feldspar and biotite are very rare or absent elsewhere in the metagabbro. The interior of the body is comprised of locally foliated and isoclinally folded metagabbro cut by numerous dikes of granite pegmatite up to 10 m wide.

Mineral assemblages are locally variable. The most common rock type is dominated by numerous large (0.5–3 mm) porphyroblasts of manganiferous almandine, strongly zoned from spessartine-rich cores to spessartine-poor rims. Included in the garnets are small crystals of epidote, edenitic hornblende, plagioclase, and rare omphacite. The garnets are embedded in a very fine-grained (0.1–10 μm) symplectitic matrix of intimately intergrown hornblende, plagioclase, and clinopyroxene. They are separated from this matrix by narrow (~200–300 μm) coronal reaction bands comprised of varying amounts of plagioclase, amphibole, in most cases magnetite, and in some cases orthopyroxene (Fig. 1). For reasons detailed below, these textures are believed to arise from reactions between garnet and omphacitic clinopyroxene. Samples collected in the vicinity of large dikes of postkinematic

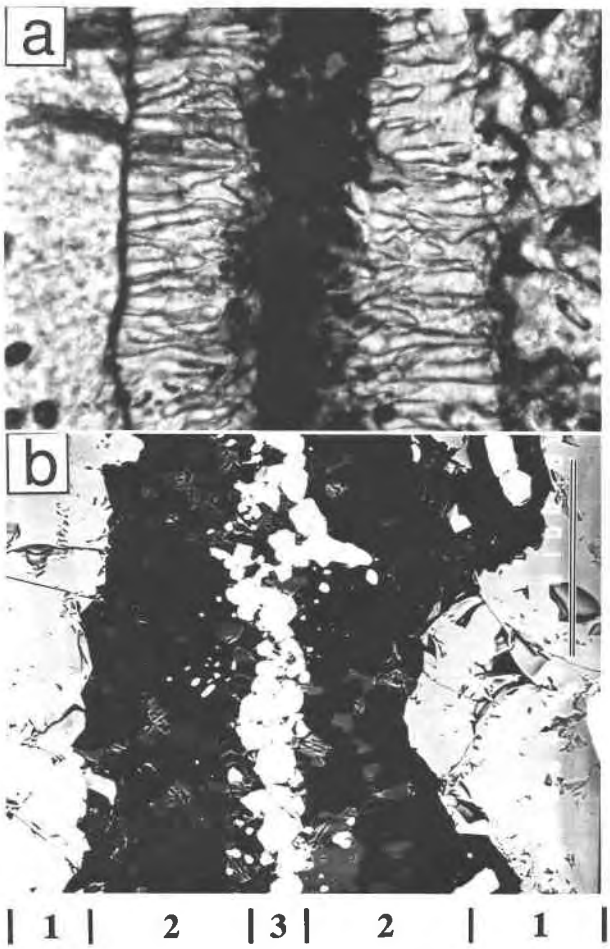

Fig. 3. Textures produced by garnet-fluid reaction along fracture in sample SS2. (**a**) Photomicrograph. Central zone of Mag (black) is separated from Alm (at left and right) by a vermicular intergrowth of Fe-Prg (darker gray) and Lab (lighter gray). Long dimension of image is 300 μm. (**b**) Backscattered-electron image. Numerals at bottom identify layers as follows: 1 = Alm; 2 = Lab (black) + Fe-Prg (gray); 3 = Mag. Scale bar at top right is 100 μm long.

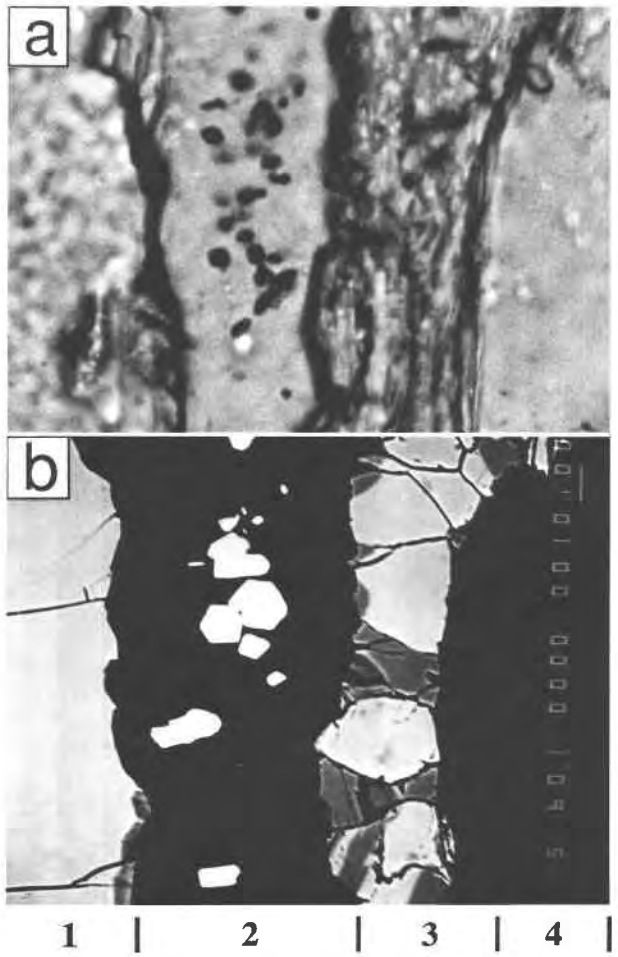

Fig. 4. Textures produced by garnet-quartz reaction in sample SS2. (**a**) Photomicrograph. Qtz (right) is adjacent to layer of Opx + Aug (darker gray); Alm (left) is adjacent to layer of Olg (lighter gray) speckled with scattered crystals of Mag (black). Long dimension of image is 160 μm. (**b**) Backscattered-electron image. The contrast with **a** in the abundance and grain size of magnetite reflects the extent of variation within the sample. Numerals at bottom identify layers as follows: 1 = Alm; 2 = Olg (black) + Mag (white); 3 = Opx (light gray) + Aug (dark gray); 4 = Qtz. Scale bar at top right is 10 μm long.

pegmatite often show a matrix assemblage enriched in hornblende at the expense of clinopyroxene and plagioclase, and many of these samples contain garnets in which more than one resorption event is made evident by a concentric repetition of the sequence of zones of coronal products. In some specimens, one finds pods of polycrystalline quartz that are free of plagioclase and amphibole but that contain slightly more manganiferous garnets surrounded by coronas of plagioclase, magnetite, orthopyroxene, and clinopyroxene (Fig. 2). These quartz-rich volumes may be remnants of quartz veins introduced into the gabbro prior to its metamorphism. Further petrographic and chemical description of the Whitt Ranch rocks may be found in Moseley (1977) and in Harris (1986).

On the basis of the regional geologic setting, the petrologic features noted above, and the thermobarometric data of Schwarze (1990), the geologic evolution of the Whitt Ranch metagabbro is believed to include this sequence of events: (1) gabbro crystallization and veining by quartz; (2) metamorphism to ~650 °C at 6–8 kbar accompanied by polyphase deformation; (3) static reheating and hydration of the entire body to ~600 °C at 2–3 kbar; and (4) additional local episodes of static reheating and hydration, restricted to the vicinity of late pegmatite dikes.

Petrography and mineral chemistry of coronas

Garnet reaction textures in the Whitt Ranch metagabbro are of three types: (1) reaction between garnet and a metamorphic fluid penetrating transcurrent fractures (Fig. 3); (2) reaction between garnet and quartz (Fig. 4); and

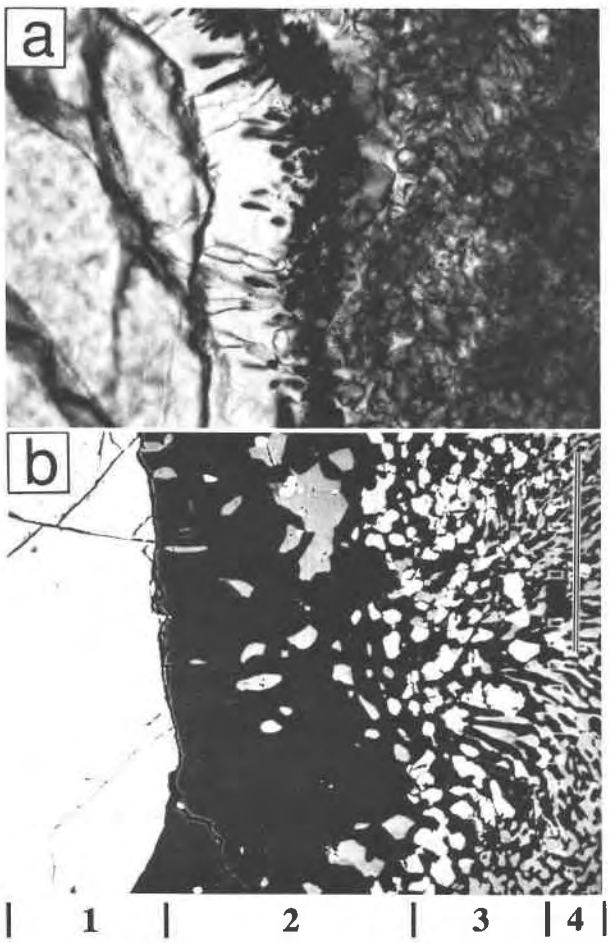

Fig. 5. Textures produced by garnet-omphacite reaction in sample SS2. (**a**) Photomicrograph. Alm (at left) is surrounded by a layer of Lab (white) with sparse elongate crystals of Fe-Prg (light gray); this is ringed by Mag (black); material to the right of the Mag is a layer of intergrown Opx + Olg + Mg-Hbl (with a narrow band of the amphibole immediately adjacent to the magnetite layer), and a layer of very fine-grained Olg + Na-Aug + Mg-Hbl (slightly darker material at right). Boundary between the two outermost layers is indistinct in this view because they are so fine grained, but each occupies about half of the dark region to the right of the Mag. Long dimension of image is 750 μm. (**b**) Backscattered-electron image. The contrast with **a** in the thickness of the reaction band and the layer modes reflects the extent of variation within the sample. Numerals at bottom identify layers as follows: 1 = Alm; 2 = Lab (black) + Fe-Prg (gray) + minor Mag (white); 3 = Opx (white) + Mg-Hbl (gray) + Olg (black); 4 = Na-Aug (gray) + Mg-Hbl (gray) + Olg (black). Scale bar at top right is 100 μm long.

(3) reaction between garnet and omphacite (Fig. 5). All three reaction textures may be present in a single thin section, and in fact, individual garnet crystals lying astride an interface between a quartz-rich volume and a clinopyroxene-rich volume commonly exhibit all three reaction bands at different places along the garnet's periphery.

Modal proportions of phases in the product layers were obtained by an image-analysis technique that digitized backscattered-electron images of the product zone, segregated phases according to their intensities in the image, and computed relative areas of all phases in the image. Multiple determinations were made, proportions in three to eight separate areas were evaluated, and the mean and standard deviation of the measurements are reported.

Compositions were obtained by electron microprobe analysis using wavelength-dispersive techniques. Data were collected with an accelerating potential of 15 kV, a sample current of 15 nA on brass (or 10 nA for feldspar), and counting times of 40 s for each element. Data reduction employed the empirical correction scheme of Albee and Ray (1970). Natural and synthetic silicates and oxides were used as standards. In most cases, at least three analyses were made of each phase in each layer. Representative individual analyses are reported in the tables that follow, but idealized compositions based on the average of several analyses (also tabulated below) were used in all calculations. The garnet analyses selected for inclusion in the tables and used for the transport calculations are from points ~100 μm away from the edges of garnet crystals. Because the crystals are zoned and partially resorbed, analyses at these locations best represent the composition of the garnet involved in the corona-forming reaction, insofar as they are as near to the crystal rim as is possible without encountering interference from the effects of intracrystalline diffusion engendered by the resorption reaction. In the following petrographic descriptions, nomenclature for amphibole follows Hawthorne (1983), with Fe^{2+}/Fe^{3+} ratios fixed by renormalizing, on the basis of 22 O and 2 OH, the sum of all cations except K, Na, and Ca to a total of 13. Pyroxene nomenclature conforms to Morimoto et al. (1988). These abbreviations are used in tables and figures: Alm = almandine; Aug = augite; Fe-Prg = ferroan pargasite; Lab = labradorite; Mg-Hbl = magnesio-hornblende; Mag = magnetite; Na-Aug = sodian augite; Olg = oligoclase; Omp = omphacite; Opx = orthopyroxene; Qtz = quartz.

Garnet-fluid reaction textures. Garnets that were fractured prior to the resorption event display symmetric bands of reaction between the garnet and the metamorphic fluid penetrating the fracture (Fig. 3). These bands consist of a central layer of magnetite separated from the garnet by a fine-grained symplectitic intergrowth of plagioclase and amphibole crystals, both elongated in the direction perpendicular to the fracture walls. Although in some cases the amphibole crystals extend across the entire reaction zone, in many instances one end of an amphibole crystal will be in contact with the magnetite layer, and the crystal will taper to a point or terminate more bluntly before reaching the garnet at the wall of the fracture. Plagioclase in these reaction bands is labradorite; its composition varies little, in contrast to plagioclase in garnet-quartz and garnet-omphacite reaction bands. Amphibole crystals are ferroan pargasite; they are too small to permit the detection of zoning along their lengths. From one hand sample to another, mineral compositions are

TABLE 1. Compositions and proportions of minerals in garnet-fluid reaction texture

	Alm	Lab	Mag	Fe-Prg
SiO_2	38.7	53.7	n.d.	42.1
Al_2O_3	21.5	29.6	0.28	15.9
FeO*	25.6	0.35	91.6	12.4
MgO	6.23	n.d.	n.d.	12.7
MnO	0.31	n.d.	n.d.	0.08
TiO_2	0.09	n.d.	0.17	1.14
CaO	7.65	11.5	n.d.	11.4
Na_2O	n.d.	5.03	n.d.	2.93
K_2O	n.d.	n.d.	n.d.	0.05
Total	100.1	100.0	92.1	98.7
Modal %		69.7	10.2	20.0
±1 esd		0.5	0.1	0.6

Note: Values in upper part of table are in wt% of oxides; n.d. = not present at levels above detection limit.
* All Fe reported as FeO.

TABLE 2. Compositions and proportions of minerals in garnet-quartz reaction texture

	Alm	Olg	Mag	Opx	Aug	Qtz
SiO_2	38.3	62.1	n.d.	51.0	52.7	
Al_2O_3	21.1	23.6	0.30	0.23	0.66	
FeO*	24.8	0.36	90.4	30.3	12.2	
MgO	4.58	n.d.	n.d.	15.8	12.0	
MnO	3.29	n.d.	n.d.	2.08	0.83	
TiO_2	0.14	n.d.	0.09	0.03	0.04	
CaO	7.82	4.89	n.d.	0.57	21.4	
Na_2O	n.d.	8.80	n.d.	n.d.	0.66	
K_2O	n.d.	n.d.	n.d.	n.d.	n.d.	
Total	100.0	99.8	90.8	100.0	100.5	
Idealized formulas used in modeling						
Si	3.00	2.75	0.00	1.99	2.00	1.00
Al	1.96	1.25	0.00	0.01	0.03	0.00
Fe	1.63	0.00	3.00	0.99	0.36	0.00
Mg	0.49	0.00	0.00	0.92	0.70	0.00
Ca	0.67	0.25	0.00	0.03	0.85	0.00
Na	0.00	0.75	0.00	0.00	0.04	0.00
O	12	8	4	6	6	2
Modal %		63.3	5.0	17.8	13.9	
±1 esd		1.5	0.8	1.0	1.0	

Note: Values in upper part of table are in wt% of the oxide; in lower part, elements not used in the model are excluded and values are atoms per formula unit; n.d. = not present at levels above detection limit.
* All Fe reported as FeO.

nearly uniform, but proportions of phases in the product zone may change markedly. Table 1 presents electron microprobe analyses and mineral modes of the products of a representative garnet-fluid reaction in sample SS2.

Garnet-quartz reaction textures. Where garnet adjoined quartz prior to the resorption event, reaction has produced coronal structures consisting of an inner layer of sodic plagioclase + minor magnetite surrounded by an outer layer of orthopyroxene + augite (Fig. 4). Feldspar composition changes systematically and gradually across the layer: plagioclase adjacent to garnet (typically andesine, $\sim An_{35}$) is more calcic than plagioclase adjacent to pyroxene (typically oligoclase, $\sim An_{18}$). In some coronas, augite crystals may be slightly more abundant near the contact of the pyroxene and plagioclase layers than they are at the opposite edge of the pyroxene layer. Although mineral compositions are nearly uniform from one hand sample to another in these reaction bands, the proportions of product phases are somewhat variable from rock to rock. In some samples, layers of plagioclase and pyroxene are nearly equal in width; in others, the plagioclase may be as much as twice as thick as the pyroxene layer. The volume percentage of orthopyroxene in the pyroxene layer ranges from ~50% in some samples to 100% in others. Table 2 presents electron microprobe analyses and mineral modes of the products of the representative garnet-quartz reaction from sample SS2 that is imaged in Figure 4b.

Garnet-omphacite reaction textures. Reaction bands that now separate garnet from an extremely fine-grained (0.1–10 μm) symplectitic intergrowth of sodian augite + oligoclase + magnesio-hornblende are believed to have arisen by reaction of garnet with an omphacitic clinopyroxene. This belief is founded upon three observations. First, plagioclase crystals in these intergrowths are in optical continuity over polygonal areas 1–4 mm in diameter, indicating that the intergrowths are pseudomorphs after a coarser-grained phase. When viewed petrographically under crossed nicols, the rock's texture takes on the appearance of an equigranular mosaic typical of high-grade mafic metaigneous rocks. Second, the field relations, bulk composition, and textures of the Whitt Ranch metagabbro are closely analogous to those of eclogitic metamafic rocks in the northwestern Llano Uplift described by Wilkerson et al. (1988) in which omphacitic clinopyroxenes have been only partially reconstituted as very similar (although coarser) vermicular intergrowths of sodian augite and plagioclase (cf. Fig. 2 of Wilkerson et al., 1988). Third, some of the garnets in the Whitt Ranch occurrence preserve inclusions of omphacite close in composition to that found as coarse primary crystals in the eclogite remnants.

In contrast to the garnet-fluid and garnet-quartz reaction bands described above, the garnet-omphacite reaction bands display substantial mineralogic variation from rock to rock. The principal differences are in the arrangement and relative proportions of orthopyroxene and hornblende. In one specimen in particular (sample SS2), the garnet-omphacite reaction bands exhibit a striking variety of product assemblages and modes. Some reaction bands contain an outer layer of abundant orthopyroxene intergrown with oligoclase and magnesio-hornblende, separated from the garnet by an inner layer rich in labradorite with minor ferroan pargasite and minute amounts of magnetite (Fig. 5b). In other reaction bands, a nearly monomineralic layer of magnesio-hornblende (often incorporating a sharp internal break in composition) is interposed between the inner and outer layers (Figs. 6a–6c). When this central amphibole layer is present, the amounts of orthopyroxene and oligoclase in the outer layer are reduced, and the amount of magnesio-hornblende in the outer layer is augmented; also, small amounts of magnetite are sometimes concentrated near the interface between the inner labradorite-rich layer and

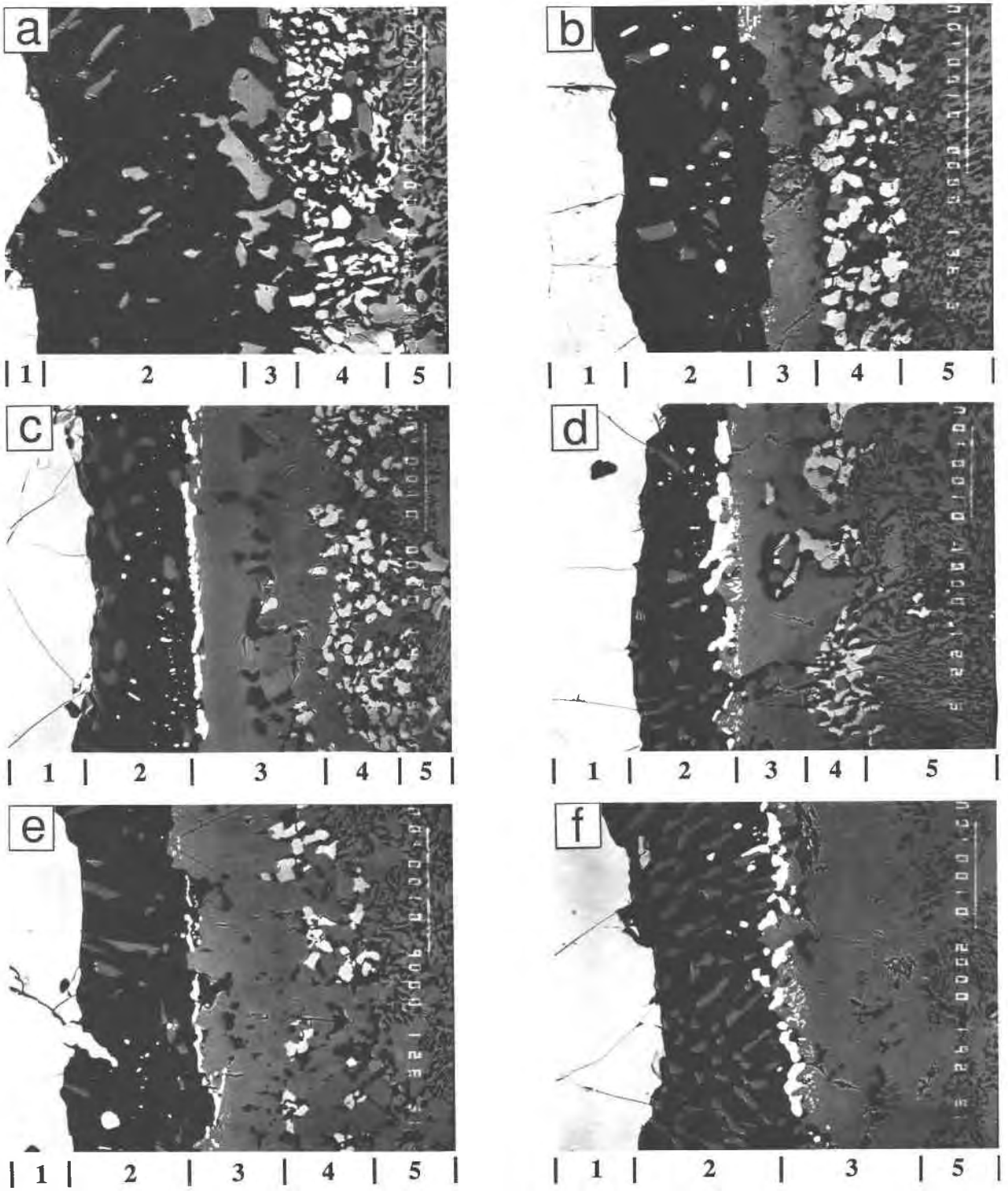

Fig. 6. Variation of garnet-omphacite reaction textures in sample SS2. Backscattered-electron images. Scale bars at top right are 100 μm long. Numerals at bottom identify layers as follows: 1 = Alm; 2 = Lab (black) + Fe-Prg (gray) + Mag (white); 3 = Mg-Hbl (gray) + Olg (black); 4 = Opx (white) + Mg-Hbl (gray) + Olg (black); 5 = Na-Aug (gray) + Mg-Hbl (gray) + Olg (black). The images from **a** through **f** are interpreted as the result of progressive replacement of Opx and Lab by Mg-Hbl in reactions occurring at the interface between layers 2 and 3 and at the interface between layers 3 and 4. This interpretation suggests that an initial increase in the proportion of Mg-Hbl in layer 3 (**a**) leads to a nearly monomineralic layer of Mg-Hbl (**b**) and (**c**) that engulfs Opx (**d**) and (**e**) and eventually eliminates it (**f**). A concurrent increase in the proportion of Fe-Prg within layer 2 is also noticeable.

TABLE 3. Compositions and proportions of minerals in garnet-omphacite reaction texture

	Alm	Lab	Fe-Prg	Opx	Olg	Mg-Hbl	Omp
SiO_2	39.5	53.8	42.8	52.4	61.6	45.5	55.0
Al_2O_3	21.9	30.0	13.6	0.29	24.5	9.15	8.10
FeO*	25.5	0.31	13.6	24.9	0.26	12.0	5.78
MgO	7.20	n.d.	12.7	21.1	n.d.	13.8	9.83
MnO	0.14	n.d.	0.04	0.14	n.d.	n.d.	0.05
TiO_2	0.02	n.d.	0.80	n.d.	n.d.	2.11	0.11
CaO	6.57	11.5	11.5	0.44	5.40	11.5	15.3
Na_2O	n.d.	4.90	2.80	0.04	8.57	2.21	5.54
K_2O	n.d.	n.d.	0.03	n.d.	0.02	0.13	n.d.
Total	100.8	100.5	97.9	99.3	100.4	96.4	99.7
Idealized formulas used in modeling							
Si	3.00	2.40	6.08	1.99	2.77	6.69	2.00
Al	1.98	1.60	2.50	0.02	1.23	1.59	0.35
Fe	1.66	0.00	1.66	0.78	0.00	1.48	0.17
Mg	0.78	0.00	2.64	1.19	0.00	3.02	0.51
Ca	0.58	0.60	1.79	0.02	0.23	1.81	0.58
Na	0.00	0.40	0.83	0.00	0.77	0.63	0.38
O	12	8	23	6	8	23	6
Modal %		43.3	3.5	10.0	34.7	8.5	
±1 esd		1.9	0.6	1.7	2.7	0.7	

Note: Values in upper part of table are in wt% of the oxide; in lower part, elements not used in the model are excluded and values are atoms per formula unit; n.d. = not present at levels above detection limit.
* All Fe reported as FeO.

the central amphibole layer. In many bands, orthopyroxene is nearly or completely absent, oligoclase is sparse, and magnesio-hornblende dominates the outermost coronal layer (Figs. 6d–6f). A continuum of textures intermediate between those of Figures 5b and 6f is observed in a single thin section of sample SS2.

Most garnet-omphacite reaction bands exhibit a sharp discontinuity in plagioclase composition near the center of the band: feldspar in the inner plagioclase-rich layer is approximately An_{60}, whereas feldspar in and near the outer layers rich in hornblende ± orthopyroxene averages An_{23}. This change, barely perceptible as lighter and darker regions in the backscattered-electron image of the plagioclase layer in Figure 5b, coincides with an abrupt change in the compositions of the associated amphibole. Amphibole in the inner labradorite-rich layer has higher Al-Si and Fe-Mg ratios than amphibole in the orthopyroxene + magnesio-hornblende + oligoclase layer, and intermediate compositions characterize hornblende where it is found in central monomineralic layers. In Figure 5b, the sharp boundary between the different compositions of amphibole and plagioclase, which lies within layer 2, does not coincide with the edge of the orthopyroxene-bearing layer. Textural details in the inner coronal zone of labradorite + ferroan pargasite resemble those in the garnet-fluid reaction bands: both feldspar and amphibole are elongated in the direction perpendicular to the garnet surface, and amphibole crystals are usually rooted in the magnetite layer (if it is present), tapering and often terminating before reaching the garnet surface (Fig. 1).

For the metagabbro body as a whole, orthopyroxene-free coronas are much more common than their orthopyroxene-bearing counterparts. Even in samples in which some coronas contain orthopyroxene, other coronas may not. Garnet-omphacite reaction bands in proximity to quartz-rich regions of these rocks are more likely to include abundant orthopyroxene and to lack monomineralic amphibole layers than are similar reaction bands more distant from quartz-rich regions.

Table 3 presents electron microprobe analyses and product mineral modes for the representative garnet-omphacite reaction band from sample SS2 that is imaged in Figure 5b, along with the average analysis of an inclusion of omphacite in garnet from sample 13.

Ancillary reaction textures. Three additional reactions in which garnet is not directly involved are also evident in rocks of the Whitt Ranch metagabbro. Most significant is the breakdown reaction of omphacite to a fine-grained symplectite of oligoclase + sodian augite + magnesio-hornblende. In contrast to all other reactions in the rock, this reaction has generated textures without strong spatial organization. As in the eclogite remnants described by Wilkerson et al. (1988), it probably reflects in situ replacement of the omphacite by an assemblage of minerals

TABLE 4. Compositions and proportions of minerals in symplectite replacing omphacite

	Olg	Na-Aug	Mg-Hbl
SiO_2	66.0	52.8	47.1
Al_2O_3	21.7	2.00	9.86
FeO*	0.42	7.33	12.2
MgO	n.d.	14.3	14.5
MnO	n.d.	0.09	0.10
TiO_2	n.d.	0.06	0.64
CaO	2.68	21.9	12.1
Na_2O	8.95	0.77	1.99
K_2O	n.d.	n.d.	n.d.
Total	99.8	99.3	98.5
Modal %	46.7	45.2	8.1
±1 esd	4.1	4.3	5.6

Note: Values in upper part of table are in wt% of the oxide; n.d. = not present at levels above detection limit.
* All Fe reported as FeO.

of lower density. It is probable that this reaction proceeded simultaneously with the corona-forming reactions, because both represent static hydration and reequilibration at lower pressures. Table 4 presents electron microprobe analyses of the phases in symplectites in sample SS2 that are believed to be pseudomorphs after an original omphacite matrix in which the garnets of that rock were formerly embedded.

Two additional subsidiary reactions have also taken place: where quartz and magnetite were once in contact with omphacite, monomineralic reaction rims of clinopyroxene (around quartz) and of hornblende (around magnetite) are observed. Both of these monomineralic reaction bands are volumetrically inconsequential.

Origin of the coronal textures

The three dissimilar garnet resorption reactions represent three distinct responses to the same reheating and hydration event. Differences among the reactions are evidently the result of variations in the local chemical environment at the scale of a few tens of micrometers, indicating that the extent of chemical exchange, at least for some components, may be highly restricted. As noted in the review above, many previous attempts to account quantitatively for coronal reaction textures have relied upon the dubious assumption that chemical exchange is so severely restricted that the reaction zones may be treated as isochemical subsystems. The following discussion of reaction mechanisms will test the validity of that assumption in the Whitt Ranch coronas and will establish that none of the reactions can be treated as isochemical. We then evaluate the extent to which these reaction zones must be in chemical communication with one another or with other reactions taking place in the rock. That information will then be used to relax the restriction of isochemistry present in Joesten's (1977) steady-state diffusion model, taking the approach of Johnson and Carlson (1990). This will lead to fully quantitative descriptions of the origin of the coronal reaction textures in the Whitt Ranch metagabbro as the products of open-system diffusion-controlled reaction.

Reaction mechanisms

Evidence for diffusional kinetic controls. Fisher (1977, p. 383) set forth the following criteria for the recognition of textures produced by diffusion-controlled reactions: "... diffusion-controlled structures characteristically have a strong spatial organization, with well-defined mineral zones showing sharp changes in compositions at zone boundaries, all arranged in an orderly sequence of increasing or decreasing chemical potential." As illustrated in Figures 3, 4, and 5, all of the garnet resorption reactions in the Whitt Ranch metagabbro possess strong spatial organization and sharply defined zone boundaries. The data in Tables 1, 2, and 3 confirm sharp changes at the zone boundaries in mineral compositions and modes, and therefore in bulk compositions. The systematic arrangement of phases in terms of the chemical potentials of the diffusing components will become apparent below, when diffusion models presuming such an arrangement are shown to replicate the arrangement and proportions of phases in the coronal reaction textures. Therefore, in the analysis that follows, intergranular diffusion will be presumed to exert the predominant kinetic control on the formation of these textures.

The kinetic role of the metamorphic fluid. The influence of the metamorphic fluid on the reaction kinetics deserves careful consideration. Metasomatic reactions driven by massive infiltration of fluids are evidently restricted to a shell extending about 30 m inward from the margins of the metagabbro body. Substantial amounts of alkalis have been imported into this shell from the surrounding quartzofeldspathic gneiss, producing assemblages including alkali feldspars and biotite that are anomalous by comparison to the assemblages in the interior of the body.

Although material transport dominated by bulk motion of a fluid brine was probably restricted to the metasomatic shell, there is direct evidence that garnet resorption reactions in the interior of the metagabbro body were triggered by the introduction of aqueous fluids along fractures and grain boundaries. Some thin sections are cut by anastamosing curvilinear veinlets, 1–3 mm wide, composed predominantly of relatively coarse crystals of hornblende, plagioclase, or both. Garnet crystals within a few hundred micrometers of these veinlets, unlike others slightly further away, have undergone two separate resorption events, as indicated by concentric double reaction bands. In some instances, the secondary (smaller) corona does not extend completely around the periphery of the garnet, but is instead restricted to the side of the garnet closest to the veinlet. A secondary corona of this type is faintly visible around the garnet remnant in Figure 1, outlined by a narrow zone of magnetite within the hornblende-plagioclase symplectite. Microtextures such as these, combined with the observation that rocks in which all garnets show multiple resorption events are found only near large pegmatite dikes, establish that fluid access initiated at least the secondary garnet resorption episodes. The petrologic evidence cited above for a regionally extensive hydration event at low pressures leads to the conclusion that fluid played a similar role in activating the primary resorption event that has affected all of the garnets in the metagabbro body.

Nevertheless, there is no evidence that the kinetics of fluid motion or the diffusion of fluid components along fractures or grain boundaries are rate-controlling factors in the generation of these coronal textures. For example, in garnet-omphacite reaction bands like that of Figure 5b, assemblages in the reaction zones do become progressively less hydrous inward toward the garnet, but it would be erroneous to infer from this that the coronal structure reflects the kinetics of fluid transport, because an equally impressive coronal structure is evident in the completely anhydrous assemblages of the garnet-quartz reaction

bands. Also, because reaction bands along fractures maintain uniform width instead of tapering inward, and because they show no longitudinal differences in mineral assemblage, it is apparent that fluid access along the length of fractures is substantially more rapid than ionic diffusion along grain boundaries perpendicular to the fracture walls. Finally, it will be shown below that diffusion models treating the chemical potentials of H_2O and O_2 as externally controlled parameters satisfactorily replicate the observed reaction textures, indicating that the kinetics of their transport does not play an essential role in the development of the coronas.

Estimates of material transport

Any analysis of the material transport involved in metamorphic reactions relies upon an assessment of the material balance between reactants and products. Thompson (1959, p. 428–430) points out that statements regarding the introduction or removal of material are meaningless without a clear specification of the frame of reference, but that all choices of reference frame can provide equally correct descriptions of the material transport. The most appropriate frame of reference for the analysis of diffusion-controlled reactions is difficult to choose, however, because reaction textures do not, in general, preserve indisputable evidence for or against (1) any particular position for the original interface between reactants, (2) volume changes, and (3) gains or losses of individual components. Two of these three sources of indeterminacy must be removed in order to produce an explicit description of the reaction, but definitive petrologic means of eliminating any of them are rare.

The resolution of this ambiguity is one of the most formidable obstacles to rigorous analysis of material transport in rocks. Previous attempts to calculate material balance in coronal textures or reaction zones have necessarily, but arbitrarily, assumed the conservation of volume, or the conservation of one or more elements, or both (e.g., Al and Si: Whitney and McLelland, 1973; Al: Thompson, 1975; Ca: Misch and Onyeagocha, 1976; Al and Si: Mongkoltip and Ashworth, 1983; Al: Johnson and Carlson, 1990) or have assumed the location of the original interface on the basis of sharp mineralogical discontinuities (e.g., Thompson, 1975, p. 329–330). In this article, gains and losses of individual components are calculated over the complete range of possible locations for the original interface between reactants by assuming conservation of volume in an inert-marker reference frame. For the modeling of diffusion, we have chosen estimates for positions of the original interfaces that correspond with boundaries between Al-rich and Al-poor layers in the reaction bands and with discontinuities in the compositions of amphibole and plagioclase.

Conservation of volume. Although large changes in the volume of the solid are likely in reactions dominated by devolatilization (see, e.g., Thompson, 1975), there may be a sound theoretical basis for a close approximation to constant-volume replacement during diffusion metasomatism involving other types of reactions (Carmichael, 1987). Careful examination of the resorption textures in the Whitt Ranch body revealed no evidence of a volume increase, such as the disturbance of structures in the surrounding fabric or outward displacements of garnet fragments separated by reaction bands developed along fractures. Likewise, nothing was seen in the textures that would preclude nearly constant-volume replacement. Thus it appears, in the light of Carmichael's (1987) theory and our petrographic observations, that the coronal reactions in the Whitt Ranch metagabbro are reasonably approximated by constant-volume replacement in an inert-marker reference frame.

We have examined in reconnaissance the effects of possible volume changes on the calculations to be presented below. If one presumes small changes in volume, less than a few percent, one calculates shifts of similar magnitude in the transport of elements, which lead in turn to minor modifications in the calculated relative diffusivities of elements required to form the coronal textures. Such changes do not, however, affect our fundamental conclusion that the coronas constitute open diffusional systems that may evolve through time. If one presumes larger changes in volume, on the order of ± 10–20%, it becomes impossible to prescribe any set of relative diffusivities for the elements that will account quantitatively for the formation of the coronas; either the calculated proportions of phases in the coronas disagree with the observed proportions, or the observed arrangement of product phases is calculated to be diffusionally unstable, or both. Given the evidence cited above for a diffusional origin for these textures, this finding appears consistent with the notion that volume changes during corona formation were small or negligible.

Locations of original interfaces between reactants. Even under the presumption of constant-volume replacement, ambiguities in calculations of material balance arise from the fact that the original interfaces between reactants cannot be located except under favorable circumstances. For the garnet-quartz and garnet-omphacite reactions, there are no unambiguous indicators of the locations of the original interfaces between reactants. Consequently, we have calculated the material balance and modeled the intergranular diffusion over the full set of possible locations for the original interfaces. The modeling allows us to place limits on the range of possible choices for the positions of the original interfaces that are consistent with the arrangement of minerals observed in the reaction bands.

Garnet-fluid reaction. For the garnet-fluid reaction taking place along fractures present in the garnets prior to resorption, the material balance for constant-volume replacement is uniquely determined if the volume of the fracture is regarded as negligible: essentially all of the volume now occupied by products was formerly occupied by garnet. The material transport required under these circumstances is illustrated in Figure 7a. The ordinate in Figure 7 has been chosen to emphasize the degree to which

each element is conserved within the reaction band during coronal formation; it is the molar percentage of each element that is lost or gained by the reaction band, indicated by positive and negative quantities, respectively. For example, a transport percentage of +50% signifies that half the number of moles originally present in the reactants has been exported beyond the boundaries of the reaction band; a transport percentage of −50% signifies that half the number of moles now present in the products had to be imported from regions outside the boundaries of the reaction band; an element that is conserved during reaction plots at 0% on the ordinate. The abscissa in the figure, expressed as a percentage of the distance across the reaction band, is used to show (in Figs. 7b and 7c) how the calculated material balance would differ depending upon one's choice for the location of the original interface between reactants. In the case of the garnet-fluid reaction (Fig. 7a), in which almandine is present on both sides of the original interface, the calculated material transport is unrelated to the presumed position of the interface, so the lines in Figure 7a are horizontal. The nonzero transport values express the fact that this reaction is not isochemical; for this reaction band, a substantial gain of Na and substantial losses of Mg, Fe, Al, and Si are required.

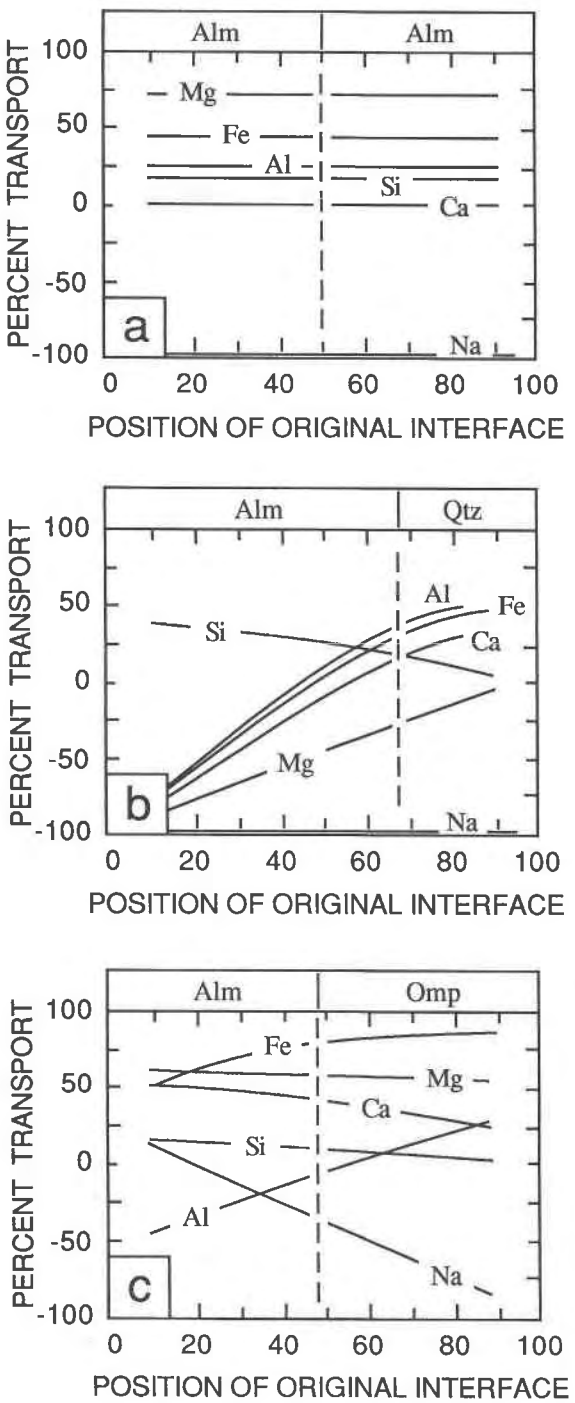

Garnet-quartz reaction. In the case of the garnet-quartz reaction, there is no petrographic evidence from which one can derive the position of the original interface between reactants; that is, there is no way to determine what fraction of the volume now occupied by plagioclase and pyroxene was formerly occupied by garnet, and what fraction by quartz. It is nevertheless clear from Figure 7b that no choice for the position of the original interface will permit this reaction to be treated as an isochemical process. In Figure 7b, an isochemical reaction would be represented by the simultaneous convergence of the lines for all elements to a value of zero for some choice of the position of the original interface. That all choices for the position of the original interface yield nonzero transport for most elements demonstrates that a closed-system diffusion model would approximate this reaction very inaccurately. The position of the original interface affects the calculated material transport in the diffusional modeling; the dashed vertical line in the figure indicates the position that is used in the examples below to estimate the amounts of material that have been transported across the outer boundary of the reaction band. That position corresponds to the contact between the plagioclase and the pyroxene layers in the product zone, that is, to the

←

Fig. 7. Material transport as a function of choice of location for original interface between reactants, assuming conservation of volume in an inert-marker reference frame. Ordinate in each diagram indicates the extent to which each element is conserved within the reaction band; it is the percentage of each element that is lost (positive values) or gained (negative values) by the reaction band (see text). Abscissa is percentage of distance across the reaction band, with 0% representing the edge of the reaction band in contact with the garnet. All three reactions require substantial import and export of material, regardless of one's choice for the position of the initial interface between reactants. Dashed vertical lines indicate the positions of the original interfaces between reactants that were used in the calculations of material balance for the examples of diffusional modeling that appear in Table 7.

contact between the Al-rich and Al-poor product layers. (The successful diffusion models below are consistent with placing the original interface near this layer contact, just inside the pyroxene layer.)

Garnet-omphacite reaction. Figure 7c demonstrates the impossibility of accurately representing the garnet-omphacite reaction as an isochemical replacement. As in Figure 7b, there is no point along the abscissa for which all transport values converge to zero, so the reaction cannot be isochemical. Regardless of the position one chooses for the original interface between reactants, substantial amounts of material must be transported across the boundaries of the reaction band as the corona forms. Once again, there is no petrographic evidence for the location of the original interface between reactants, and the dashed vertical line in the figure indicates the position that is used in the examples below to estimate the amounts of material that have been transported across the outer boundary of the reaction band. The position is again chosen to fall at the contact between the Al-rich (labradorite + ferroan pargasite) and Al-poor (orthopyroxene + magnesio-hornblende + oligoclase) product layers, at the discontinuity in compositions of the amphibole and plagioclase. (The successful diffusion models below are consistent with placing the original interface near this layer contact, just inside the orthopyroxene-bearing layer.)

Material balances. Under the assumption of constant-volume replacement, any choice for the location of the original interface in each reaction band uniquely specifies the amount of material that has been imported into or exported from the reaction band. Using the locations indicated by the dashed lines in Figure 7, Table 5 casts these estimates of the material balance as the number of moles of each element that is imported into or exported from the reaction bands, per mole of garnet resorbed. These time-integrated boundary fluxes will be incorporated below into a quantitative model for the intergranular diffusion within the garnet-quartz and garnet-omphacite reaction bands.

It is unlikely that rocks of the Whitt Ranch metagabbro represent closed systems at any scale. Table 5 shows that the three garnet-resorption reactions cannot compensate for one another: all three are net sources of Si, Fe, and Ca; all three are net sinks for Na. The other reactions taking place in the rock cannot account for all of the material lost and gained by the garnet reactions. Although the omphacite-breakdown reaction is a source rather than a sink for Na, it (like all three garnet resorption reactions) is a source for Si, Fe, and Ca. The subsidiary reactions producing clinopyroxene around quartz and hornblende around magnetite could serve as minor sinks for Si, Fe, and Ca, but these reactions are volumetrically insignificant. These considerations suggest that Si, Fe, and Ca are not conserved within the rock at the scale of hand samples and possibly at much larger scales. This conclusion is not surprising considering the ample petrologic evidence for substantial chemical interaction of the rocks with fluids at all scales.

TABLE 5. Boundary fluxes

	Garnet-fluid	Garnet-quartz	Garnet-omphacite
	(moles per mole of garnet resorbed)		
Si	0.53	0.82	0.57
Al	0.48	0.58	−0.29
Fe	0.75	0.43	1.53
Mg	0.53	−0.21	1.02
Ca	0.00	0.07	0.69
Na	−0.42	−0.83	−0.40

Open-system diffusion models

The hypothesis of a diffusional origin for the garnet-quartz and garnet-omphacite reaction bands can be tested by constructing a quantitative open-system model based upon that of Joesten (1977), as modified by Johnson and Carlson (1990). The modeling below seeks an answer to this question: Is there any range of possible values for the relative rates of intergranular diffusion of Na, Ca, Fe, Mg, Si, and Al for which the observed arrangement of product layers is stable with respect to continual diffusion? If there is none, then either the diffusion model is oversimplified and unable to represent the natural reaction accurately, or these textures originated by some other process. If such a range of relative diffusivities does exist, then it is of geologic interest to try to determine the relative magnitudes of those diffusivities and their dependence upon the intensive parameters of metamorphism.

Steady-state diffusion models. The model of isochemical, steady-state diffusion of Joesten (1977) evaluates, from the observed arrangement and measured compositions of minerals in a reaction band, the range of ratios of intergranular diffusion coefficients for which that reaction band could stably form. This is accomplished by solving a large system of simultaneous linear equations that describes the fluxes and reactions within the growing reaction band; those equations impose upon the reaction band the constraints of local equilibrium, mass balance, and nonequilibrium thermodynamics. Joesten's (1977) article provides a lucid exposition of the approach and of the system of equations required, using a hypothetical reaction as an example. Because Joesten's model has also been abstracted in each of the later papers that sought to apply it to natural coronal textures (Nishiyama, 1983; Grant, 1988; Johnson and Carlson, 1990), details of the model will not be reiterated here.

The only undetermined quantities in the system of equations are the phenomenological coefficients (L_{ij}) that relate the flux (J_i) of a component to the chemical-potential gradients ($d\mu_j/dx$) for each of the n_c diffusing components in the fundamental diffusion equation:

$$J_i = \sum_{j=1}^{n_c} - L_{ij} \frac{d\mu_j}{dx}. \quad (1)$$

Like all earlier approaches except that of Grant (1988), this treatment neglects, when evaluating the flux of one

element, the contributions of gradients in the chemical potentials of other elements; thus all cross coefficients (those L_{ij} for which $i \neq j$) are taken as zero, and L_{ii} is written more simply as L_i. In addition, this treatment, like all earlier ones, regards the L_i as constants, despite the fact that each is proportional to the concentration of the element in the intergranular medium and the fact that those concentrations must vary across the reaction band in the presence of chemical-potential gradients for the diffusing components. There is some suggestion in the results of the modeling below that while treatment of the L-ratios as constant within a given reaction texture may be a valid approximation, variations in concentrations of elements in the intergranular medium among different types of coronal reaction bands may be large enough, even in a single sample, to affect values of the L-ratios appreciably. (For discussion of the implications of considering L-ratios to vary across a reaction band, consult Joesten, 1977, p. 661–665.)

In order to allow for the transport of materials beyond the boundaries of the reaction band as required by the material-balance calculations, Joesten's (1977) model must be modified. The method of Johnson and Carlson (1990) is used again here. This method integrates into Joesten's system of equations a set of boundary-flux equations that specify the amount of each element lost or gained by the reaction band. Those amounts are obtained from estimates of material balance, as illustrated above for the case of the Whitt Ranch coronas.

Application to the Whitt Ranch coronas. The garnet-quartz reaction imaged in Figure 4b, in which both reactants are essentially Na-free, has been modeled in the diffusional system CaO-FeO-MgO-$AlO_{3/2}$-SiO_2 by treating the chemical potentials of $NaO_{1/2}$, $HO_{1/2}$, and O as externally controlled (i.e., determined by equilibria beyond the boundaries of the reaction band). The garnet-omphacite reaction imaged in Figure 5b has been modeled in the diffusional system $NaO_{1/2}$-CaO-FeO-MgO-$AlO_{3/2}$-SiO_2 by treating the chemical potentials of $HO_{1/2}$ and O as externally controlled. In the garnet-omphacite corona, labradorite was modeled as a phase distinct from oligoclase, and ferroan pargasite was modeled as a phase distinct from magnesio-hornblende; gradations in the composition of plagioclase across all zoned layers were ignored, and average compositions were used. In both cases, fluxes at the outer boundary of the reaction band were computed on the basis of the positions for the original interfaces shown in Figure 7, and fluxes across the inner boundary (the contact with the central garnet crystal) were taken as zero. The equations used to describe these reaction bands appear in Table 6.[1]

The observed arrangement of phases in both reaction bands was calculated to be diffusionally stable over a substantial range of possible values for the ratios of phenomenological coefficients in this open-system model. Table 7 presents an example of the calculated interface reactions and diffusional transport for each of the reaction bands. The examples chosen are situations in which the L-ratios are near unity; these sets of L-ratios are therefore representative of the minimum differences in the phenomenological coefficients that are required in order to generate diffusionally stable solutions. Numerous diffusionally stable solutions also exist that involve greater differences between pairs of the phenomenological coefficients.

We emphasize, however, that attempts to treat these coronal textures as if they were isochemical are inadequate. Such a treatment of the garnet-omphacite textures fails to identify any region in L-ratio space for which the given arrangement of product assemblages is diffusionally stable. Likewise, although an isochemical approach to the garnet-quartz textures leads to the calculation of stable assemblage zonations over a restricted range of L-ratios, those solutions yield calculated modes that depart significantly from the actual modes. It is evident that proper specification of the boundary fluxes is an essential prerequisite to accurate estimation of the ratios of phenomenological coefficients.

To explore further the dependence of estimates for the ratios of phenomenological coefficients on the boundary fluxes, the Whitt Ranch coronas were modeled over the entire range of possible choices for the positions of the original interfaces between reactants. Not surprisingly, for some values of these choices, for which garnet represented small fractions of the reactant volume, no set of possible values for the ratios of phenomenological coefficients was found that produces diffusionally stable assemblage zonations matching the observed reaction bands. Less extreme values produced small regions in L-ratio space that would be consistent with the observed bands, but these regions occupy different portions of the space for different choices of the material balance.

Values of *L*-ratios. Much of the interest in coronal textures centers on extracting from them the actual ratios of phenomenological coefficients, knowledge of which would make it possible to evaluate the relative rates of intergranular diffusional transport during metamorphism. In the Whitt Ranch coronas, however, there are large irregularly shaped regions of L-ratio space for which the observed reaction bands are computed to be diffusionally stable; these regions shift somewhat when different values for the boundary fluxes are employed. Consequently, few generalities can be drawn from the modeling. For the boundary fluxes presented in Table 5, the garnet-quartz coronas suggest $L_{Fe} \approx L_{Si} > L_{Ca} > L_{Mg}$ (with L_{Al} poorly constrained), whereas the garnet-omphacite coronas suggest $L_{Na} \approx L_{Fe} > L_{Mg} \geq L_{Si} \geq L_{Ca} \geq L_{Al}$.

Joesten (1977) points out that in some reaction bands, the modal proportions of phases in some layers or zones depend upon the ratios of phenomenological coefficients, so that measurement of the modes sometimes permits

[1] A copy of Table 6 may be ordered as Document AM-91-457 from the Business Office, Mineralogical Society of America, 1130 Seventeenth Street NW, Suite 330, Washington, DC 20036, U.S.A. Please remit $5.00 in advance for the microfiche.

TABLE 7. Examples of diffusion models for corona formation

	Garnet-quartz reaction band				Garnet-omphacite reaction band		
Coefficients of interface reactions (moles per mole of garnet resorbed)							
	Reaction interface*				Reaction interface*		
	1–2	2–3	3–4		1–2	2–3	3–4
Alm	−1.000	0	0	Alm	−1.000	0	0
Olg	1.183	−0.092	0	Lab	1.126	−0.017	0
Mag	0.543	−0.346	0	Fe-Prg	0.059	−0.027	0
Opx	0	0.067	0.414	Opx	0	0.006	0.398
Aug	0	0.095	0.273	Olg	0	0.020	0.792
Qtz	0	0	−2.514	Mg-Hbl	0	0.027	0.038
				Omp	0	0	−1.959
Si	−0.253	−0.070	1.143	Si	−0.064	−0.038	0.672
Al	0.481	0.111	−0.012	Al	0.030	0.029	−0.349
Fe	0.000	0.939	−0.509	Fe	1.561	0.002	−0.033
Mg	0.490	−0.128	−0.573	Mg	0.623	−0.015	0.412
Ca	0.374	−0.060	−0.245	Ca	−0.202	0.007	0.886
				Na	−0.500	−0.003	0.103
Fluxes across layers (moles per mole of garnet resorbed)							
	Layer*				Layer*		
	2	3	4		2	3	4
Si	−0.253	−0.323	0.820	Si	−0.064	−0.102	0.570
Al	0.481	0.592	0.580	Al	0.030	0.059	−0.290
Fe	0.000	0.939	0.430	Fe	1.561	1.563	1.530
Mg	0.490	0.363	−0.210	Mg	0.623	0.608	1.020
Ca	0.374	0.315	0.070	Ca	−0.202	−0.196	0.690
				Na	−0.500	−0.503	−0.400
Product modes (vol. %)							
	Observed	Model			Observed	Model	
Olg	63.3	63.2		Lab	43.3	45.4	
Mag	5.0	5.0		Fe-Prg	3.5	3.6	
Opx	17.8	17.7		Opx	10.0	10.5	
Aug	13.9	14.0		Olg	34.7	33.3	
				Mg-Hbl	8.5	7.2	

Note: Garnet-quartz example gives results calculated for $L_{Si}/L_{Al} = 1$, $L_{Si}/L_{Ca} = 1$, $L_{Si}/L_{Fe} = 0.316$ ($= 10^{0.5}$), and $L_{Si}/L_{Mg} = 1$. Garnet-omphacite example gives results calculated for $L_{Si}/L_{Al} = 10$, $L_{Si}/L_{Ca} = 1$, $L_{Si}/L_{Fe} = 0.1$, $L_{Si}/L_{Mg} = 0.1$, and $L_{Si}/L_{Na} = 1$.

* Numbers for interfaces and layers match those in Figures 4b and 5b.

one to deduce particular values of the L-ratios that would produce the measured proportions of phases. But, as the example in Joesten (1977, p. 658) illustrates, the modal proportions in a reaction band will be invariant over the field of L-ratios unless one or more phases is present in a pair of adjacent layers. Thus in the case of the garnet-quartz and garnet-omphacite coronas of the Whitt Ranch metagabbro, in which no two layers share a common phase, the modal proportions and the relative layer widths calculated by the model are independent of the postulated ratios of phenomenological coefficients.

In the Whitt Ranch occurrence, however, one might consider taking another approach to restricting the range of possible ratios for the phenomenological coefficients. Because both the garnet-quartz and the garnet-omphacite reactions take place simultaneously in the same small volume of rock, the actual values of the L-ratios might be expected to lie in the intersection of the ranges for each of the individual reactions, insofar as they represent diffusion at the same temperature and pressure. That expectation would be based upon the assertion that the principal determinants of the phenomenological coefficients are the intrinsic mobility of each diffusing species, and intensive parameters such as the temperature, pressure, and chlorinity of the intergranular fluid; it would regard as negligible the effects of differing concentrations of elements in the intergranular fluid that might result from local buffering by different assemblages.

In the Whitt Ranch coronas, there is indeed overlap in the ranges of ratios for the phenomenological coefficients for which the individual reaction bands are calculated to be diffusionally stable, but the L-ratios within the range of overlap require the ratio L_{Si}/L_{Na} in the garnet-omphacite corona to be 10 or greater. Such ratios may be inconsistent with qualitative notions of the relative mobility of these elements (e.g., Misch and Onyeagocha, 1976; Whitney and McLelland, 1973; Mongkoltip and Ashworth, 1983). If instead one considers L-ratios that lie nearer to the centers of each of the two individual regions of diffusionally stable solutions in L-ratio space, those inconsistencies disappear.

As an alternative, then, one might consider the possibility that the relative rates of diffusion for Mg, Fe, Ca, Al, and Si may have been slightly different in the garnet-

quartz coronas than in the garnet-omphacite coronas, rather than lying in the range of overlap. It is conceivable that the mineral assemblages in the two coronas might have locally buffered the concentrations of diffusing species to different values. For example, the intergranular fluid at least at one end of the garnet-quartz reaction band was saturated with silica, but the entire garnet-omphacite reaction band was probably undersaturated in silica, as the analysis presented in the following section indicates. Because the phenomenological coefficients are proportional to local concentrations in the intergranular fluid, and because those local concentrations are probably different in the two types of coronas, it is plausible that the L-ratios may vary appreciably from one coronal type to the other. The most impressive difference between the most likely relative L-values for the two reactions is that the L-value assigned to Si is greater in the garnet-quartz reaction, which is consistent with the idea that a higher concentration of silica in the garnet-quartz reaction fluid augments the value of the phenomenological coefficient there. To the extent that concentrations must also vary across each individual reaction band, this inference invalidates the assumption that the L-ratios may be treated as constant across the band. However, the fact that diffusionally stable solutions (using constant L-ratios) for individual coronas are found over wide ranges of L-ratio space suggests that the effects of variable concentration across a given reaction band introduce acceptably small errors into the calculations.

Evolution of coronal assemblages

The variety of garnet-omphacite reaction textures shown in Figures 5 and 6 suggests that these reaction bands may have undergone a history more complex than just a single-stage steady-state diffusion episode. All of the textures shown in Figures 5 and 6 are reasonably interpreted as representing reaction bands in which orthopyroxene was originally present over nearly half the width of the band, but in which hornblende has subsequently replaced orthopyroxene along only one edge of the orthopyroxene-bearing layer, the edge closer to the central garnet crystal. This observation requires explanation, because it poses the problems of identifying the cause of the replacement reaction and accounting for its variable degree and its selective and directional nature.

One conceivable explanation for the elimination of orthopyroxene is simply that during the waning stages of the static metamorphic event responsible for the formation of the coronas, temperatures dropped sufficiently to cause orthopyroxene to become unstable with respect to hornblende in the presence of an aqueous fluid. There are, however, several reasons to regard this explanation as unlikely, or at least incomplete. First is the preservation in most garnet-quartz coronas of orthopyroxene in intimate association with plagioclase, the same phase with which it appears to react in the garnet-omphacite coronas. A second argument against declining temperature as an exclusive explanation for the elimination of orthopyroxene is the evidence for unidirectional replacement. In all cases, only one edge of the orthopyroxene-bearing zone (the one nearer the garnet crystal) is subject to the replacement reaction; by contrast, orthopyroxene-rich regions in contact with the polymineralic matrix of sodian augite + oligoclase + magnesio-hornblende appear unaffected (Figs. 6b–6e). Third, because the entire range from incipient to complete replacement is found within a single thin section (and, in some cases, on opposite sides of a single garnet crystal), one cannot call upon local variations in temperature to account for the local variation in degree of replacement; some sort of additional kinetic factors must be invoked.

An alternative explanation is suggested by the association of the garnet-omphacite coronas containing orthopyroxene with quartz-rich regions of the rock, and by the lack of reaction between orthopyroxene and plagioclase in many garnet-quartz coronas. These observations are consistent with the notion that the stability of orthopyroxene depends sensitively upon the local activity of silica and other components in the intergranular fluid. The foregoing material-balance calculations indicate that both the garnet-omphacite reaction and the simultaneous reaction of omphacite to sodian augite + oligoclase + magnesio-hornblende are sources of silica and other components. If, as the omphacite-breakdown reaction in the matrix surrounding the garnets progresses toward completion, it ceases to function as a local source or sink for some components, then their activities at the outer boundary of the reaction band will change. This will perturb the boundary fluxes at the outer limit of the reaction band, which may in turn alter the internal diffusive fluxes in such a way that the orthopyroxene-bearing assemblage is rendered diffusionally unstable relative to hornblende. We hypothesize, therefore, that the variability and the unidirectionality of the orthopyroxene replacement textures arise from local changes with time in the boundary fluxes, changes that arise from the progressive exhaustion of the omphacite-breakdown reaction as that reaction nears completion.

This hypothesis has been tested by calculating the effects of changes in the boundary fluxes of Si and Al, the dominant components that are respectively produced and consumed by the omphacite-breakdown reaction. The boundary fluxes of these two elements were altered in the directions and proportions that would simulate the gradual elimination of the omphacite-breakdown reaction in the surrounding matrix, and the effects on the modal proportions of minerals in the reaction band were calculated for several different values of the boundary fluxes. Table 8 presents the results of those calculations. As the hypothesis predicts, these changes in the boundary fluxes lead to greater amounts of hornblende in both product layers, at the expense of orthopyroxene and plagioclase. For sufficiently large changes in the boundary fluxes (rightmost column in Table 8), the calculations predict the eventual elimination of orthopyroxene as a diffusionally stable member of the product assemblage, mirroring

the progressive changes displayed in Figures 5b and 6a–6f.

These changes with time in the product modes and assemblages are directly analogous to those revealed, with equally explicit visual evidence, in the olivine-plagioclase coronas of metagabbros of the Adirondacks (Johnson and Carlson, 1990). In the Adirondack coronas, there is petrographic confirmation that the changes in product assemblages are caused by the gradual exhaustion of one of the reactants, calcic plagioclase, as a source for Ca and Si. In the Whitt Ranch rocks, a similar role is apparently played by the gradual elimination of the breakdown reaction of omphacite as a source for Si and a sink for Al. These reaction textures that show evolution of products over time have an important feature in common: one of the original reactants is undergoing chemical modification simultaneously with the corona-forming reaction. This modification affects the boundary fluxes and the overall material balance, shifting the internal fluxes and altering the internal reactions. In such circumstances, a steady-state diffusion model that presumes an unchanging assemblage of product phases may lead to erroneous results.

TABLE 8. Effects on garnet-omphacite products of elimination of omphacite-breakdown reaction

	Boundary fluxes (moles per mole of garnet resorbed)			
Si	0.57	0.66	0.75	0.80
Al	−0.29	−0.37	−0.45	−0.49
Fe	1.53	1.53	1.53	1.53
Mg	1.02	1.02	1.02	1.02
Ca	0.69	0.69	0.69	0.69
Na	−0.40	−0.40	−0.40	−0.40
	Vol. % of products			
Lab	45.4	35.7	32.8	30.1
Fe-Prg	3.6	5.2	5.8	6.4
Opx	10.5	3.9	1.9	0.0
Olg	33.3	34.1	34.4	34.6
Mg-Hbl	7.2	21.1	25.1	28.8

Conclusions

This investigation confirms, in wholly different petrologic circumstances, the inference drawn by Johnson and Carlson (1990) that closed-system approaches to diffusion-controlled reaction textures may yield incorrect analyses of the nature, extent, and rates of element transport by intergranular diffusion. It demonstrates that nonequilibrium transport models for the origin of the Whitt Ranch coronas can be constructed by specifying boundary fluxes from material-balance calculations, and that such models are quantitatively consistent with the arrangement and modes of mineral assemblages in the reaction bands. It suggests that the range of possible ratios for the phenomenological coefficients determined by a diffusion model may be very poorly constrained, because the petrographically observable features of the reaction band are often not highly sensitive to those ratios. Despite the overlap in the ranges of possible values for the ratios of phenomenological coefficients in the two coronal types in the Whitt Ranch metagabbro, the actual values in the two coronal types may have been slightly different, reflecting differences between the two coronal environments in the concentrations of dissolved species in the intergranular fluid.

A more general conclusion, again familiar from our earlier work, stands out clearly: there is a misleading simplicity in many coronal textures. Although they preserve both reactants and products and the spatial relationships among them, many harbor subtle but unequivocal indications of extraordinarily complex origins. In particular, changes in the product assemblages with time, as illustrated in Figures 5b and 6a–6f, severely limit the applicability of steady-state models, which presume that a given reaction band originates with all product layers present at infinitesimal thickness and then simply enlarges over time. Whenever one or more of the reactants undergoes chemical changes as the corona-forming reaction progresses, the coronal assemblages may evolve with time. This potential for modification over time of product mineral assemblages emphasizes the risk of assuming that the assemblages one observes in a diffusion-controlled texture were present throughout the rock's diffusional history.

Because this study focuses attention on the complex chemical interactions between local corona-forming reactions and their surroundings, it amplifies the admonition of one of the earliest workers on these textures, namely Sederholm (1916, p. 142), who remarked: "Often . . . interpretations [of coronal and similar textures] seem to lie so close at hand, that it appears only necessary to grasp a pen and write them down on paper. But, as we have found, . . . the reactions between mineral substances derived from the adjacent minerals have been complicated by transfer of material from greater distances, thus increasing the difficulty of an interpretation." This study and its predecessor (Johnson and Carlson, 1990) both argue that the starting point for such interpretations must be an attempt to solve quantitatively the perplexing problems of the nature and magnitudes of the boundary fluxes and of the degree to which they remain constant or change as reaction progresses.

Acknowledgments

We wish to extend special thanks to Susan Harris, whose Master's thesis on the Whitt Ranch rocks under the supervision of the senior author uncovered a number of crucial observations and demonstrated, in an early attempt to develop diffusion models for the Whitt Ranch coronas, the necessity of treating such textures as the products of open-system reaction. We are also grateful to Elizabeth Schwarze, who generously contributed her thermobarometric estimates for the Whitt Ranch and other localities prior to their publication and who provided the microprobe analysis of the omphacite inclusion that appears in Table 3. Lee Whitt graciously allowed access to his property for field work. The constructive criticisms offered in reviews by Ray Joesten, Tom Foster, and John Brady materially improved both the content and presentation of the article, and their contributions are gratefully acknowledged. Portions of this work were supported by NSF grant EAR-8804717 to W.D.C., Nicholas Walker, and Sharon Mosher. The Geology Foundation of the University of Texas helped to defray costs of publication.

References cited

Albee, A.L., and Ray, L. (1970) Correction factors for electron probe microanalysis of silicates, oxides, carbonates, phosphates and sulfates. Analytical Chemistry, 42, 1408–1414.

Bebout, G.E., and Carlson, W.D. (1986) Fluid evolution and transport during metamorphism: Evidence from the Llano Uplift, Texas. Contributions to Mineralogy and Petrology, 92, 518–529.

Brady, J.B. (1977) Metasomatic zones in metamorphic rocks. Geochimica et Cosmochimica Acta, 41, 113–125.

Carlson, W.D. (1989) The significance of intergranular diffusion to the mechanisms and kinetics of porphyroblast crystallization. Contributions to Mineralogy and Petrology, 103, 1–24.

Carlson, W.D., and Nelis, M.K. (1986) An occurrence of staurolite in the Llano Uplift, central Texas. American Mineralogist, 71, 682–685.

Carmichael, D.M. (1987) Induced stress and secondary mass transfer: Thermodynamic basis for the tendency toward constant-volume constraint in diffusion metasomatism. In H.C. Helgeson, Ed., Chemical transport in metasomatic processes, p. 239–264. Reidel, Dordrecht, the Netherlands.

Carter, K.E. (1989) Grenville orogenic affinities in the Red Mountain area, Llano Uplift, Texas. Canadian Journal of Earth Sciences, 26, 1124–1135.

Chesworth, W. (1972) Metamorphic facies series in the Grenville province of Ontario. Tectonophysics, 14, 71–78.

Fisher, G.W. (1973) Nonequilibrium thermodynamics as a model for diffusion-controlled metamorphic processes. American Journal of Science, 273, 897–924.

——— (1975) The thermodynamics of diffusion-controlled metamorphic processes. Mass transport phenomena in ceramics, p. 111–122. Plenum, New York.

——— (1977) Nonequilibrium thermodynamics in metamorphism. Thermodynamics in geology, p. 381–403. Reidel, Boston.

Foster, C.T. (1981) A thermodynamic model of mineral segregations in the lower sillimanite zone near Rangeley, Maine. American Mineralogist, 66, 260–277.

——— (1983) Thermodynamic models of biotite pseudomorphs after staurolite. American Mineralogist, 68, 389–397.

——— (1986) Thermodynamic models of reactions involving garnet in a sillimanite/staurolite schist. Mineralogical Magazine, 50, 427–439.

Garrison, J.R., Jr., Long, L.E., and Richmann, D.L. (1979) Rb-Sr and K-Ar geochronologic and isotopic studies, Llano Uplift, central Texas. Contributions to Mineralogy and Petrology, 69, 361–374.

Grant, S.M. (1988) Diffusion models for corona formation in metagabbros from the Western Grenville Province, Canada. Contributions to Mineralogy and Petrology, 98, 49–63.

Harris, S.F. (1986) Kinetics of diffusion-controlled reactions in garnet amphibolite, Llano County, Texas, 121 p. Unpublished M.A. thesis, University of Texas at Austin, Austin, Texas.

Hawthorne, F.C. (1983) The crystal chemistry of the amphiboles. Canadian Mineralogist, 21, 173–480.

Holdaway, M.J., and Lee, S.M. (1977) Fe-Mg cordierite stability in high-grade pelitic rocks based on experimental, theoretical, and natural observations. Contributions to Mineralogy and Petrology, 63, 175–198.

Joesten, R. (1977) Evolution of mineral assemblage zoning in diffusion metasomatism. Geochimica et Cosmochimica Acta, 41, 649–670.

——— (1986a) The role of magmatic reaction, diffusion and annealing in the evolution of coronitic microstructure in troctolitic gabbro from Risor, Norway. Mineralogical Magazine, 50, 441–467.

——— (1986b) The role of magmatic reaction, diffusion and annealing in the evolution of coronitic microstructure in troctolitic gabbro from Risor, Norway: Reply. Mineralogical Magazine, 50, 474–479.

Johnson, C.D., and Carlson, W.D. (1990) The origin of olivine-plagioclase coronas in metagabbros of the Adirondack Mountains, New York. Journal of Metamorphic Geology, 8, 697–717.

Jordan, M.A. (1970) Garnetiferous metagabbro near Babyhead, Llano County, Texas, 75 p. Unpublished M.A. thesis, University of Texas at Austin, Austin, Texas.

Misch, P., and Onyeagocha, A.C. (1976) Symplectite breakdown of Ca-rich almandines in upper-amphibolite-facies Skagit Gneiss, North Cascades, Washington. Contributions to Mineralogy and Petrology, 54, 189–224.

Mongkoltip, P., and Ashworth, J.R. (1983) Quantitative estimation of an open-system symplectite-forming reaction: Restricted diffusion of Al and Si in coronas around olivine. Journal of Petrology, 24, 635–661.

Morimoto, N., Fabries, J., Ferguson, A.K., Ginzburg, I.V., Ross, M., Seifert, F.A., Zussman, J., Aoki, K., and Gottardi, G. (1988) Nomenclature of pyroxenes. American Mineralogist, 73, 1123–1133.

Moseley, M.G. (1977) Geochemistry and metamorphic history of the Whitt metagabbro, Llano County, Texas, 86 p. Unpublished M.A. thesis, University of Texas at Austin, Austin, Texas.

Mosher, S. (in press) Western extensions of Grenville Age rocks: Texas. In J.C. Reed, Jr., D.W. Rankin, P.K. Sims, W. Reynolds, and R.S. Houston, Eds., The Precambrian: U.S., Decade of North American geology centennial volume. Geological Society of America, Boulder, Colorado.

Nelis, M.K., Mosher, S., and Carlson, W.D. (1989) Grenville-age orogeny in the Llano Uplift of central Texas: Deformation and metamorphism of the Rough Ridge Formation. Geological Society of America Bulletin, 101, 876–883.

Nishiyama, T. (1983) Steady diffusion model for olivine-plagioclase corona growth. Geochimica et Cosmochimica Acta, 47, 283–294.

Ridley, J., and Thompson, A.B. (1986) The role of mineral kinetics in the development of metamorphic microtextures. Advances in Physical Geochemistry, 5, 154–193.

Schwarze, E.T. (1990) Polymetamorphism in the Llano Uplift: Evidence from geothermobarometry and compositional zoning in garnet, 275 p. Unpublished M.A. thesis, University of Texas at Austin, Austin, Texas.

Sederholm, J.J. (1916) On synantetic minerals and related phenomena. Bulletin de la Commission Geologique de Finlande, 48, 1–148.

Thompson, A.B. (1975) Calc-silicate diffusion zones between marble and pelitic schist. Journal of Petrology, 16, 314–346.

Thompson, J.B., Jr. (1959) Local equilibrium in metasomatic processes. In P.H. Abelson, Ed., Researches in geochemistry, vol. 1, p. 427–457. Wiley, New York.

Walker, N.W. (1988) U-Pb zircon evidence for 1305–1231 Ma crust in the Llano Uplift, central Texas. Geological Society of America Abstracts with Programs, 20, 205.

Whitney, P.R., and McLelland, J.M. (1973) Origin of coronas in metagabbros of the Adirondack Mts., N.Y. Contributions to Mineralogy and Petrology, 39, 81–98.

Wilkerson, A., Carlson, W.D., and Smith, D. (1988) High-pressure metamorphism during the Llano orogeny inferred from Proterozoic eclogite remnants. Geology, 16, 391–394.

Zartman, R.E. (1964) A geochronologic study of the Lone Grove pluton from the Llano Uplift, Texas. Journal of Petrology, 5, 359–408.

Manuscript received January 31, 1990
Manuscript accepted February 14, 1991